

Case Reports

Highly Metastatic Ovarian Yolk Sac Carcinoma in a Rat

Akika Sakamoto¹, Yuko Yamaguchi¹, Seiki Yamakawa², Mariko Nagatani², and Kazutoshi Tamura¹

¹ Pathology Department, Gotemba Laboratories, Bozo Research Center Inc., 1284 Kamado, Gotemba, Shizuoka 412-0039, Japan

² Hamamatsu Branch of Pathology Department, Bozo Research Center Inc., 164-2 Wada-cho, Higashi-ku, Hamamatsu, Shizuoka 435-0016, Japan

Abstract: We investigated a highly metastatic ovarian yolk sac carcinoma in a 52-week-old female Crl:CD(SD) rat. Macroscopically, the present case had severe ascites, bilateral ovarian masses and numerous nodules in the abdominal and thoracic cavities. Histopathologically, these masses and nodules were generally composed of two types of cells mimicking a parietal and visceral yolk sac. The parietal cells were round to polygonal, contained eosinophilic droplets and were arranged in nests and cords in the eosinophilic matrix. Both the intracytoplasmic droplets and the matrix were stained positively with PAS. The visceral cells were cylindric, and proliferated in papillary and tubular patterns and occasionally formed Shiller-Duval body-like structures. In the dissemination sites, the neoplastic cells proliferated on the surface of the various tissues and often infiltrated into deeper parts of the tissues. Immunohistochemically, both neoplastic cells were positive for α -fetoprotein and keratin, and the eosinophilic matrix was positive for laminin. Ultrastructurally, the parietal cells had dilated rough endoplasmic reticulum, which were filled with electron-lucent laminated structures. The visceral cells had poorly to moderately developed intracytoplasmic organelles and were interconnected with desmosomes. Taken together, the present tumor was diagnosed as yolk sac carcinoma arising from the ovary and was characterized by not only high metastasis but also invasive infiltration with biphasic proliferation of the parietal and visceral cells. (DOI: 10.1293/tox.24.81; J Toxicol Pathol 2011; 24: 81–85)

Key words: Yolk sac carcinoma, ovary, highly metastatic, spontaneous, rat

Yolk sac carcinoma, also known as endodermal sinus tumor, is a rare spontaneous neoplasm of germ cell origin in rodents^{1–5}, although it can be experimentally induced in rats and mice^{6,7} by implantation of an extraembryonic part or whole egg cylinder under the kidney capsule and by displacement of the visceral yolk sac with or without mouse sarcoma virus into the placenta after fetectomy. Both spontaneous and induced yolk sac tumors are composed of cells mimicking a parietal and/or visceral yolk sac. They are characterized by secretion of PAS-positive hyaline matrix in the parietal yolk sac cells and by production of α -fetoprotein (AFP) in the visceral yolk sac cells. In this report, we described a spontaneous rat ovarian yolk sac carcinoma with a highly metastatic and invasive nature.

The animal was a 52-week-old female Crl:CD(SD) rat (Charles River Laboratories Japan, Inc., Kanagawa, Japan) used in a treated group from a toxicological study. No relationship between the present tumor development and the

test chemical treatment was suggested. The animal was housed individually in a wire mesh cage under controlled conditions (23 ± 3 °C room temperature, $50 \pm 20\%$ relative humidity and 12-h light/dark cycle) and given CRF-1 diet (CLEA Japan, Inc., Shizuoka, Japan) and tap water *ad libitum*.

Clinically, the animal began to exhibit bloating from 50 weeks of age and was euthanized due to deterioration of condition, with decreased spontaneous movement and bradypnea 2 weeks later. Macroscopically, in the abdominal cavity, retention of reddish transparent ascites (ca 100 mL), dark-brownish masses in both ovaries ($25 \times 25 \times 25$ mm in the right, $15 \times 15 \times 15$ mm in the left) and many yellowish-white nodules (up to $5 \times 5 \times 5$ mm) on the visceral tissues was observed. Several similar nodules were also found in the thoracic cavity, and the largest one ($20 \times 10 \times 5$ mm) was present in the mediastinum, involving the thymus and mediastinal lymph nodes (Fig. 1).

After complete necropsy, all tissues were fixed in 10% neutral-buffered formalin and embedded in paraffin. Thin sections from all tissues were stained with hematoxylin and eosin (HE). Additional sections from the tumors were stained by periodic acid-Schiff (PAS) and Masson's trichrome (MT) staining and were also subjected to immunohistochemistry for AFP by the labeled streptavidin-biotin



Fig. 1. Macroscopic findings of spontaneous yolk sac carcinoma in a rat. Dark-brownish masses in the ovaries (arrowhead) and numerous yellow-whitish nodules in the abdominal and thoracic cavities.

method using a SAB-PO kit (Nichirei, Tokyo, Japan) and for keratin and laminin by the peroxidase-labeled polymer method using an Envision kit (Dako, Kyoto, Japan). The primary antibodies used were goat anti-AFP polyclonal antibody (1:150, Santa Cruz Biotechnology, Santa Cruz, CA, USA), rabbit anti-keratin polyclonal antibody (1:500, Dako, Carpinteria, CA, USA) and rabbit anti-laminin polyclonal antibody (1:500, DAKO Denmark A/S, Glostrup, Denmark).

For electron microscopic examination, small pieces of tissues from the ovarian masses that were originally fixed with 10% neutral formalin were refixed with 0.5% glutaraldehyde and 1.5% paraformaldehyde, postfixed with 1% osmium tetroxide and embedded in epoxy resin (Oken Shoji, Tokyo, Japan). Ultrathin sections were stained with uranyl acetate and lead citrate and examined under a JEM-100 CXII transmission electron microscope (Nippon Denshi, Tokyo, Japan).

Histologically, both ovaries were almost completely replaced by neoplastic cells, showing similar histological pictures, and the normal ovarian tissue scarcely remained in the peripheral area of the tumor. The tumors were composed of cells mimicking a parietal and visceral yolk sac (Fig. 2A). Each type of the neoplastic cells proliferated with a characteristic growth pattern. The parietal cells were round to polygonal with a round to pleomorphic nucleus and intracytoplasmic eosinophilic droplets. These cells were arranged in nests or cords in an abundant eosinophilic matrix (Fig. 2B). Both the intracytoplasmic droplets and the eosinophilic matrix were stained intensively by PAS (Fig. 2C). Moreover,

tubular and small cystic structures lined by goblet cells were occasionally observed (Fig. 2D). Although hemorrhage was observed in some areas, no massive necrosis was seen. On the other hand, the visceral cells were cylindric with a round to oval nucleus and proliferated in tubular and papillary patterns with interstitial connective tissues (Fig. 2E). Single cell necrosis was frequently seen in the parietal cells and was less frequently seen in the visceral cells. In the intra-abdominal nodules, the neoplastic cells proliferated on the surface of the peritoneum and deeply invaded the parenchyma of the visceral organs and tissues including the liver, kidneys, pancreas, spleen and diaphragm (Fig. 2F). Schiller-Duval body-like structures, more apparent on MT-stained sections, characterized by a central capillary surrounded by visceral cells (Fig. 2G) and a few trophoblastic giant cells were found (Fig. 2H). Although mitotic figures were not frequently detected in the parietal and visceral cells, the neoplastic cells invaded both the ovarian capsules and the blood vessels in the periovarian tissues (Fig. 2I). Moreover, the thymus and mediastinal lymph node were involved in the neoplastic cells with focal necrosis. Immunohistochemically, both neoplastic cells were clearly positive for AFP (Fig. 3A, B) and keratin (Fig. 3C, D), and the eosinophilic matrix in the parietal cells was positive for laminin (Fig. 3E).

Ultrastructurally, the parietal cells were characterized by microvilli on the cell surface and by dilated rough endoplasmic reticulum (rERs) in the cytoplasm, whereas other intracytoplasmic organelles were not well developed in these cells. The dilated rERs were filled with electron-lucent homogenous, and occasionally laminated, structures (Fig. 4A). The tumor matrix was composed of similar materials to those observed in the dilated cisternae of rERs, but not to those of laminated structures. Conversely, the visceral cells had poorly to moderately developed intracytoplasmic organelles and well developed desmosomes (Fig. 4B). Collagenous fibers were noted in the matrix of the area of visceral cell proliferation.

The morphological characteristics of the present neoplastic cells were generally comparable to those of yolk sac tumors previously reported in rats and mice¹⁻⁵, while some immunohistochemical differences were pointed out between the present case and the previous ones. Namely, AFP was produced by visceral yolk sac cells in rodent yolk sac carcinoma reported previously^{1,7}, while parietal cells as well as visceral cells were positive for AFP in the present case. The meaning of this is obscure, and therefore, more cases and evidence is needed for discussion. In regard to immunohistochemistry for keratin, both parietal and visceral cells showed a positive reaction in the present tumor. Although there have been no available data on the immunohistochemical nature of the tumor in rodents, it is known that ovarian dysgerminoma with yolk sac components shows a positive immunohistochemical reaction for keratin as well as AFP in humans⁸. Therefore, the present tumor may provide useful information on the immunohistochemical nature of rodent yolk sac tumors.

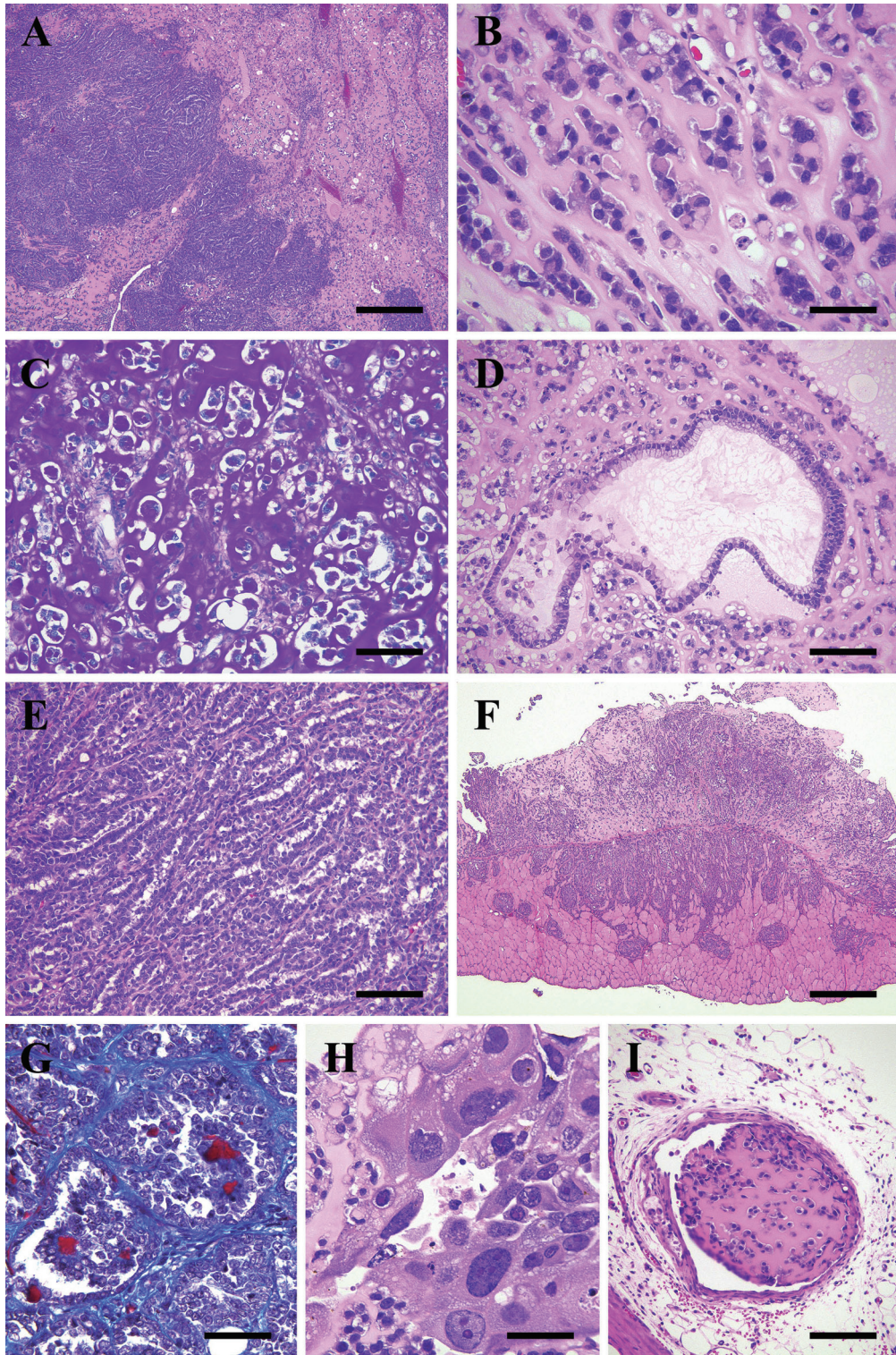


Fig. 2. Characteristic pictures of spontaneous yolk sac tumor in a rat. A: Ovarian tumors were composed of two types of cells mimicking a parietal and visceral yolk sac. HE stain, Bar = 500 μ m. B: Parietal cells arranged in a nest and cords of cells in the abundant eosinophilic matrix. HE stain, Bar = 50 μ m. C: Eosinophilic droplets in the neoplastic cells and the tumor matrix were stained positively by the PAS reaction. PAS stain, Bar = 100 μ m. D: Parietal cells formed a cyst lined by goblet cells. HE stain, Bar = 100 μ m. E: Visceral cells showed tubular and papillary proliferation. HE stain, Bar = 100 μ m. F: Metastatic focus in the diaphragm. HE stain, Bar = 500 μ m. G: Schiller-Duval body-like structures. MT stain, Bar = 50 μ m. H: Trophoblastic giant cells. HE stain, Bar = 50 μ m. I: Parietal cells invaded into the blood vessels. HE stain, Bar = 100 μ m.

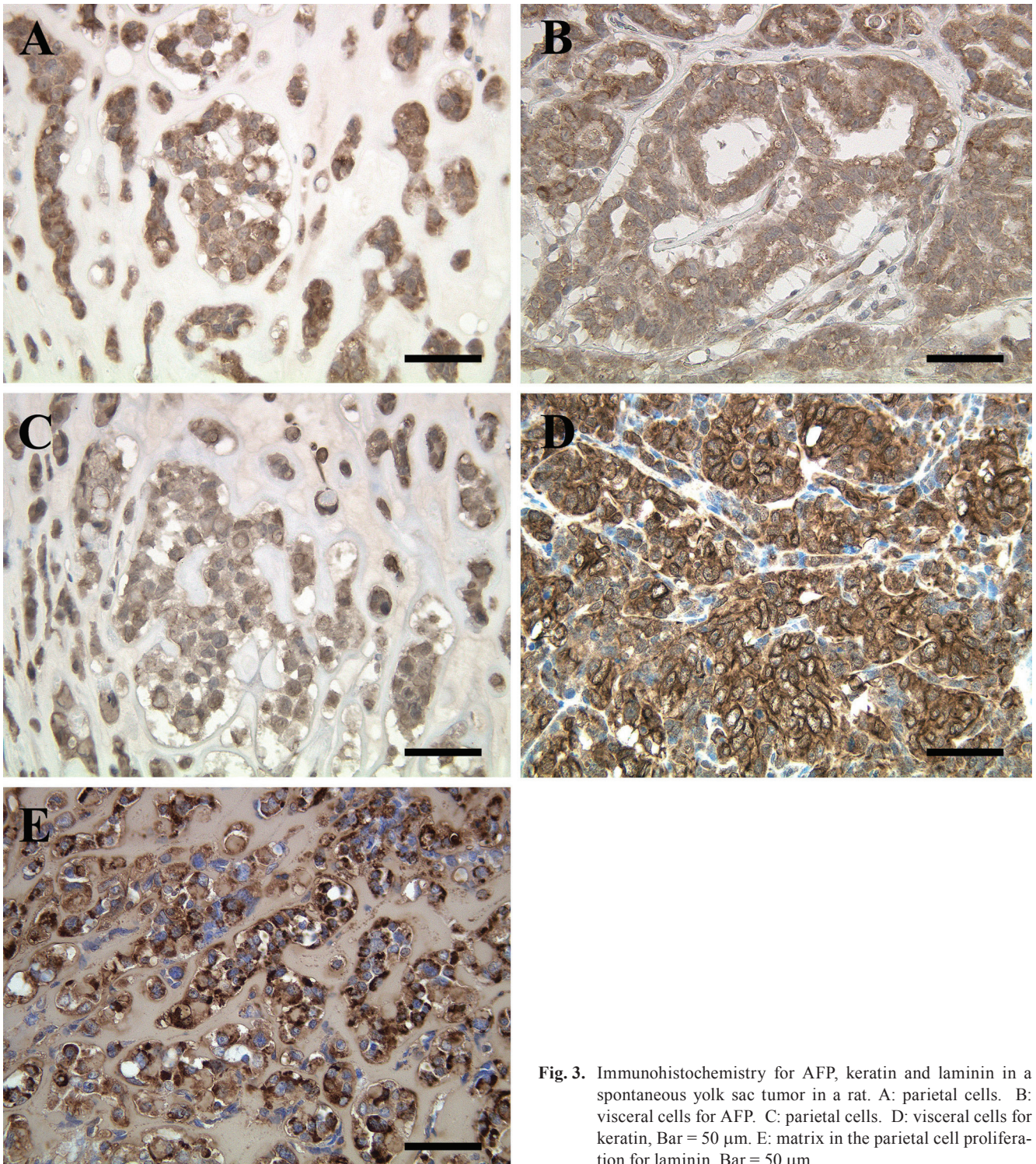


Fig. 3. Immunohistochemistry for AFP, keratin and laminin in a spontaneous yolk sac tumor in a rat. A: parietal cells. B: visceral cells for AFP. C: parietal cells. D: visceral cells for keratin, Bar = 50 μ m. E: matrix in the parietal cell proliferation for laminin, Bar = 50 μ m.

The hyaline matrix observed in the area of parietal cell proliferation showed similar characteristics to those of Reichert's membrane from a normal embryo^{9,10}, in terms of morphology and staining, and the parietal cells are considered to have that contained similar materials in the dilated rERs.

Biologically, the present tumor was highly malignant, and the neoplastic cells were extensively disseminated in

the abdominal cavity and also metastasized to distant organs via blood and lymphatic vessels, but less frequency. The neoplastic cells on the peritoneal surface frequently invaded into the deeper part of the parenchyma. Such highly invasive behavior with biphasic proliferation of the parietal and visceral cells is one of the characteristics of the present tumor. The primary site of the present tumor is considered

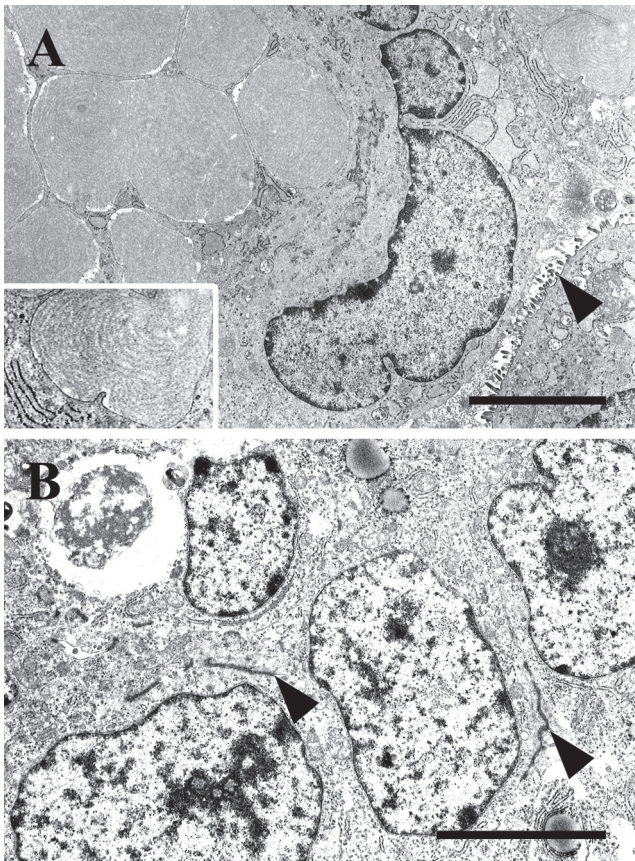


Fig. 4. Ultrastructure of neoplastic cells in a spontaneous yolk sac tumor in a rat. A: Parietal cells had microvilli on the cell surface (arrowhead) and dilated rough endoplasmic reticula filled with laminated structures in the cytoplasm (insert). Bar = 3 µm. B: Visceral cells had well-developed desmosomes (arrowhead) and slightly developed intracytoplasmic organelles. Bar = 3 µm.

to be the right ovary, since the biggest mass was observed there. However, there still remains a possibility that the present tumor developed multicentrically in both ovaries.

Germ cell tumors derived from the ovary are classified into dysgerminoma and embryonal carcinoma. Embryonal carcinoma, a totipotent tumor, is further classified into yolk sac carcinoma or choriocarcinoma (extraembryonic) and teratoma (ectoderm, mesoderm and endoderm)^{8,11}. It has been reported that inducible yolk sac carcinoma is composed of endodermal cells and contains mesenchymal, trophoblastic and mesodermal cells^{7,12}. Furthermore, in a previous report, a small yolk sac carcinoma-like focus was detected in a large immature ovarian teratoma in a rat¹³. From this evidence, it is considered that the tubular and cystic structures lined by goblet cells and trophoblastic giant cells in the present tumor may have resulted from differentiation or dedifferentiation of totipotent or endodermal cells. It is important to examine various regions of the tumor because tumors like this contain several different elements.

Taken together, the present tumor was diagnosed as

ovarian yolk sac carcinoma composed of both parietal and visceral components and was characterized by highly disseminated metastasis and invasive proliferation.

Acknowledgments: The authors thank Dr. Kunio Doi, Professor Emeritus of the University of Tokyo, for critical review and Mr. Pete Aughton, D.A.B.T., ITR Laboratory Canada Inc., for language editing of this paper.

References

1. Sobis H. Yolk sac carcinoma, rat. In: Monographs on the Pathology of Laboratory Animals 'Genital System', TC Jones, U Mohr and RD Hunt (eds), Berlin: Springer-Verlag. 127–133. 1987.
2. Frith CH, and Evans MG. Spontaneous ovarian choriocarcinoma, yolk sac carcinoma and teratoma in B6C3F1 mice: A case report. *Toxicol Pathol.* **21**: 91–98. 1993.[\[Medline\]](#) [\[CrossRef\]](#)
3. Nakazawa M, Tawaratani T, Uchimoto H, Kawaminami A, Ueda M, Ueda A, Iwakura K, Sumi N, and Kura K. Testicular yolk sac carcinoma in an aged Sprague-Dawley rat. *J Toxicol Pathol.* **11**: 203–204. 1998. [\[CrossRef\]](#)
4. Majeed SK, Alison RH, Boorman GA, and Gopinath C. Ovarian yolk sac carcinoma in mice. *Vet Pathol.* **23**: 776–778. 1986.[\[Medline\]](#)
5. Damjanov I. Yolk sac carcinoma (endodermal sinus tumor). *Am J Pathol.* **98**: 569–572. 1980.[\[Medline\]](#)
6. Sobis H, Verstuyf A, and Vandeputte M. Visceral yolk sac-derived tumors. *Int J Dev Biol.* **37**: 155–168. 1993.[\[Medline\]](#)
7. Sobis H, Van Hove L, and Vandeputte M. Trophoblastic and mesenchymal structures in rat yolk sac carcinoma. *Int J Cancer.* **29**: 181–186. 1982.[\[Medline\]](#) [\[CrossRef\]](#)
8. Parkash V, and Carcangiu ML. Transformation of ovarian dysgerminoma to yolk sac tumor: evidence for a histogenetic continuum. *Mod Pathol.* **8**: 881–887. 1995.[\[Medline\]](#)
9. Martinez-Hernandez A, Nakane PK, and Pierce GB. Intracellular localization of basement membrane antigen in parietal yolk sac cells. *Am J Pathol.* **76**: 549–560. 1974.[\[Medline\]](#)
10. Jensh RP, Koszalka TR, Jensen M, Biddle L, and Brent RL. Morphological alterations in the parietal yolk sac of the rat from the 12th to the 19th day of gestation. *J Embryol Exp Morphol.* **39**: 9–21. 1977.[\[Medline\]](#)
11. Talerman A. Germ cell tumors. *Ann Pathol.* **5**: 145–157. 1985.[\[Medline\]](#)
12. Zusman I, Zimmer A, Gdalevitch H, Yaffe P, and Pinus H. Effects of N-Methyl-N'-Nitro-N-Nitrosoguanidine and deoxycholic acid on processes of transformation of rat visceral yolk sac. *Acta Anat.* **140**: 362–368. 1991.[\[Medline\]](#) [\[CrossRef\]](#)
13. Tsubota K, Yoshizawa K, Fujihira S, Okazaki Y, Matsumoto M, Nakatsuji S and Oishi Y. A spontaneous ovarian immature teratoma in a juvenile rat. *J Toxicol Pathol.* **17**: 211–218. 2004. [\[CrossRef\]](#)